



Pergamon

Available online at www.sciencedirect.com

SCIENCE @ DIRECT®

Acta Materialia 51 (2003) 4897–4906



www.actamat-journals.com

The influence of surface structure on wetting of $\alpha\text{-Al}_2\text{O}_3$ by aluminum in a reduced atmosphere

Ping Shen *, Hidetoshi Fujii, Taihei Matsumoto, Kiyoshi Nogi

Joining and Welding Research Institute, Osaka University, 11-1 Mihogaoka Ibaraki, Osaka, 567-0047, Japan

Received 28 October 2002; received in revised form 11 June 2003; accepted 15 June 2003

Abstract

An improved sessile-drop wetting experiment was performed in this study to investigate the wettability and adhesion of molten Al on three different oriented $\alpha\text{-Al}_2\text{O}_3$ single crystals, R (011̄2), A(11̄20) and C(0001), over a wide temperature range from 800–1500 °C in a reduced Ar-3%H₂ atmosphere. It is found that the wettability and adhesion between molten Al and $\alpha\text{-Al}_2\text{O}_3$ are quite sensitive to the crystallographic orientation. The adhesion is much stronger for the molten Al on the R and A surfaces than that on the C surface. On the other hand, the adhesion on the reconstructed C-($\sqrt{3}\times\sqrt{3}$)R ± 9° surface is weaker than that on the relaxed yet unreconstructed C-(1 × 1) surface. The results suggest that in the reduced Ar-3%H₂ atmosphere, the top layers of the R and A $\alpha\text{-Al}_2\text{O}_3$ surfaces are oxygen-terminated while that of the C surface is aluminum-terminated, and the reconstructed C-($\sqrt{3}\times\sqrt{3}$)R ± 9° surface is an oxygen-deficient structure based on the results of the work of adhesion.

© 2003 Acta Materialia Inc. Published by Elsevier Ltd. All rights reserved.

Keywords: Wetting; Al; Crystallographic orientation; Surface

1. Introduction

Alumina is a technologically important oxide crystal because of its wide applications in catalysts, electronic packaging and other fields where ceramic-metal bonding is used [1–3]. Characterizations of the Al₂O₃ surface such as atomic termination, relaxation, reconstruction, domains and steps have received an increasing interest in recent years [4].

The nature of the atomic termination on the α -

Al₂O₃ surface, due to its importance in understanding and controlling the physical processes and characteristics such as film/crystal epitaxial growth, adhesion and the overlayer lattice structure of thin-film deposition [5], has been studied by many researchers using both experimental and theoretical methods, especially on the (0001) $\alpha\text{-Al}_2\text{O}_3$ surface (hereafter designated by the letter C) [5–18]. However, details of the results are quite controversial. Some studies indicate that the C surface is an oxygen-terminated structure [13–15], and others suggest it may be composed of mixed oxygen and aluminum domains with an oxygen-rich composition [16–18], while most researches, in particular, many theoretical predictions, favor

* Corresponding author. Tel./fax: +81-6-6879-8663.

E-mail address: shenping@jwri.osaka-u.ac.jp (P. Shen).

that it should be a single Al-layer termination [5–12]. An easily understood explanation for the aluminum termination is based on electrostatic considerations. As illustrated in Fig. 1, the oxygen-terminated surface is polar because there is a non-zero dipole moment left in the unit stacking sequence of the semi-infinite crystal (O-Al-Al). Therefore, the surface is expected to be very unstable. On the contrary, the aluminum-terminated surface is nonpolar, because the net dipole moment in the stacking sequence (Al-O-Al) is zero, thus, the surface should be more stable [3]. Also, there are reports that an atmosphere such as H₂ and/or water vapor may change the Al-termin-

ated C surface to an O-terminated one [10,19–23]. Previous photoemission studies of the hydroxyl-ation of the clean C surface showed a water vapor pressure of about 1-torr was sufficient to fully hydroxylate the surface [19]. Recent theoretical calculations indicate that adding one hydrogen atom per unit cell to the C surface dramatically lowers the surface free energy [10,21]. On other crystallographic planes, such as (0112) (designated by the letter R) and (1120) (designated by the letter A), controversy also exists but to a less extent (partly due to fewer studies on these faces). For example, Gignac and Williams [24] suggested that the R-plane is Al-terminated, while J.-M. Gugliel-macci et al. [16] found that the R surface, like the C, has an Al-O combined termination with an oxygen-rich composition. Others such as J. Guo et al. [5] determined that it is a single oxygen-layer termination structure. Generally speaking, despite the great interest and extensive research on the atomic termination of the α -Al₂O₃ surface, it is still an open question because there is yet no definitive experimental evidence to demonstrate that the real termination is Al or O at the top layer of the surfaces [3,7].

In this study, we examined the effect of surface structure on the wettability of the R, A and C α -Al₂O₃ single crystals by molten Al in a reduced Ar-3%H₂ atmosphere. Since the wetting is directly related to the substrate surface structure, it may provide some important information. For instance, Nogi et al. [25] demonstrated the surface structural change of diamond into graphite by investigating the wettability of molten Sn on the (100), (110) and (111) planes of diamond. In a sense, deductions from accurate wetting results may be more convincing than from some normal surface analysis techniques because wetting and adhesion are primarily related to the surface structure, in particular, the top layer atoms of the contact phases, while the normal techniques such as low-energy electron diffraction (LEED) and X-ray photoemission spectroscopy (XPS) utilize incident electron beams or X-ray as the information acquisition sources, which can easily pass into the sub-layers of the substrate surface. This situation is more serious when the large inward-relaxation of the surface atoms occurs during heating process so

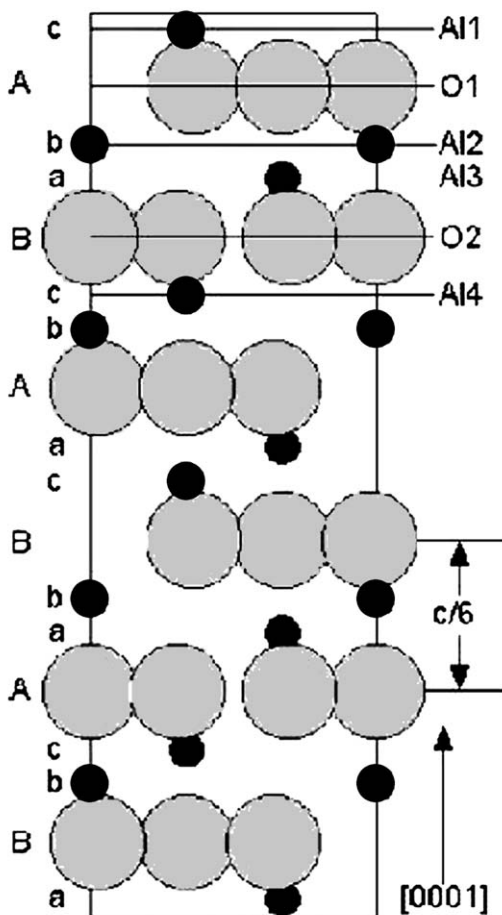


Fig. 1. Illustration of a hexagonal unit cell of (0001) α -Al₂O₃. The planes labeled by Al1, O2 and Al2 can all serve as ideal (bulk-like) termination for the (0001) surface [6].

that the underlaying atoms are very close to the top layer [4,26–27], making the distinguishing between the top-layer atoms and the second-layer atoms rather difficult.

2. Experimental procedure

The high-purity (99.99%) α -Al₂O₃ single crystals, R, A and C, used in this study were from Kyocera Co., Ltd., Japan with a size of ϕ 20 mm \times 1 mm. The surfaces were cut along their orientation planes with an error of $\pm 0.3^\circ$ and were polished to an average roughness (Ra) of less than 1 Å. The Al specimens, with a purity of 99.99%, were in the form of a wire segment weighing about 0.2 g.

An improved sessile drop method [28–29] was used in this study. In this method, the sessile drop was formed by extruding through a narrow orifice of an alumina tube and dropping onto the substrate surface. In this case, the initial oxide on the Al surface can be mechanically removed and the measured contact angles are more accurate and closer to the true contact angles of the Al/ α -Al₂O₃ system.

Fig. 2 shows a schematic of the experimental apparatus. It consists of a stainless-steel chamber with a tantalum cylindrical heater and a Mo reflector, an evacuating system with a rotary pump and a turbo molecular pump (TMP), a dropping device, a temperature program controller with a W-5%Ra/W-26%Rh thermocouple, a 10 mW He-Ne laser, a band-pass filter and a high-resolution dig-

tal camera with 2000×1312 pixels. The band-pass filter can cut all other wavelengths except for the laser beam (632 nm). Thus, the reflection light inside the chamber at high temperatures can be removed and high definition drop profiles can be obtained [30].

Before the experiment, both the α -Al₂O₃ substrate and the Al specimen were immersed in acetone and ultrasonically cleaned, then the α -Al₂O₃ substrate was placed horizontally in the chamber while the Al specimen was placed in a glass tube with a spring connector on the top of the dropping device outside the chamber. The chamber was first evacuated to about 5×10^{-4} Pa and then heated to the desired temperature in vacuum at the heating rate of 20 °C/min. After the experimental temperature was reached, the chamber was purged with a premixed high-purity Ar-3%H₂ gas purified using platinum asbestos and magnesium perchlorate. The pressure inside the chamber was raised to about 1.2 atm and the oxygen partial pressure was estimated at less than 1.1×10^{-14} Pa [31]. The Al segment was then inserted into the bottom of the alumina tube and kept for 1 min in order for it to melt and reach the experimental temperature. The molten Al was forced out from a small hole in the bottom of the alumina tube and dropped onto the α -Al₂O₃ substrate by a gradual decrease in the pressure inside the chamber to about 1.1 atm. At the same time, the initial oxide on the Al surface was mechanically removed as the liquid passed through the small hole.

As soon as the molten Al came into contact with the α -Al₂O₃ substrate, a photo was taken and defined as the drop profile at zero time. Subsequent photos were taken at time intervals of 10 s, 30 s, 1 min and 3 min. The captured photographs were analyzed by a computer using automatic image processing programs, in which the contact angle, surface tension and density could be calculated all at once which removed the operator's subjectivity.

After cooling, the solidified Al droplets were removed by etching in a 10wt.%NaOH distilled-water solution. The substrate surface profiles at the interface close to the triple junctions were measured by a Dektak 3 Surface Profilometer and observed under an optical microscope.

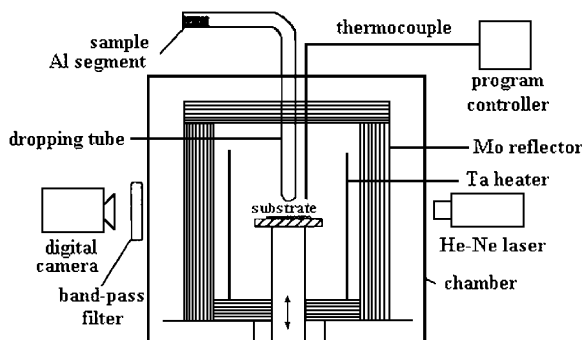


Fig. 2. Schematic of experimental apparatus.

3. Results

Fig. 3(a)–(c) show the variations in contact angles of the R, A, and C single crystals with time at temperatures from 800–1500 °C as plotted on a logarithmic time scale. It is clear that the R and A faces show a similar behavior of the contact angle versus time over the entire temperature range, while the C face exhibits a different behavior at temperatures lower than 1200 °C. The contact angle of the C face first increases with time and then reaches a constant value. The time needed to reach a constant angle decreases with temperature. The increase in the contact angle of the C face is attributed to a surface structural reconstruction from a (1×1) to a final $(\sqrt{31} \times \sqrt{31})R \pm 9^\circ$ structure as we have preliminarily reported in Ref. [32] (Here $R \pm 9^\circ$ denotes rotation by $\pm 9^\circ$), which is extremely stable at temperatures higher than 1200 °C. However, in the presence of Al, the transformation temperature shifts to a much lower value [33].

The variations in the possibly *true* contact angles of the R, A and C single crystals with temperature are shown in Fig. 4(a)–(c), respectively. Some experimental errors and linear fit results are also indicated. It should be pointed out that the possibly *true* contact angle is based on the following assumptions: the values at 30 s are the true contact angles for all the $\alpha\text{-Al}_2\text{O}_3$ single crystals, however, for the C face, the values at 30 min in the temperature range of 800–1100 °C are also employed since they represent the finally stable reconstructed $(\sqrt{31} \times \sqrt{31})R \pm 9^\circ$ structure while the values at 30 s in the same temperature range may represent the relaxed yet unreconstructed (1×1) surface structure. Such assumptions are because the initial values before 30 s may not be very accurate due to drop vibration after its breakaway from the alumina tube even if the dropping distance is short (typically less than 5 mm). Whereas, the values at a long dwelling time may be affected by surface oxidation of the molten Al at relatively low temperatures and the interfacial reaction between Al and $\alpha\text{-Al}_2\text{O}_3$ at relatively high temperatures. Actually, at relatively low temperatures, the contact angles determined at 30 s are not very different from the others in one run of the experiment for

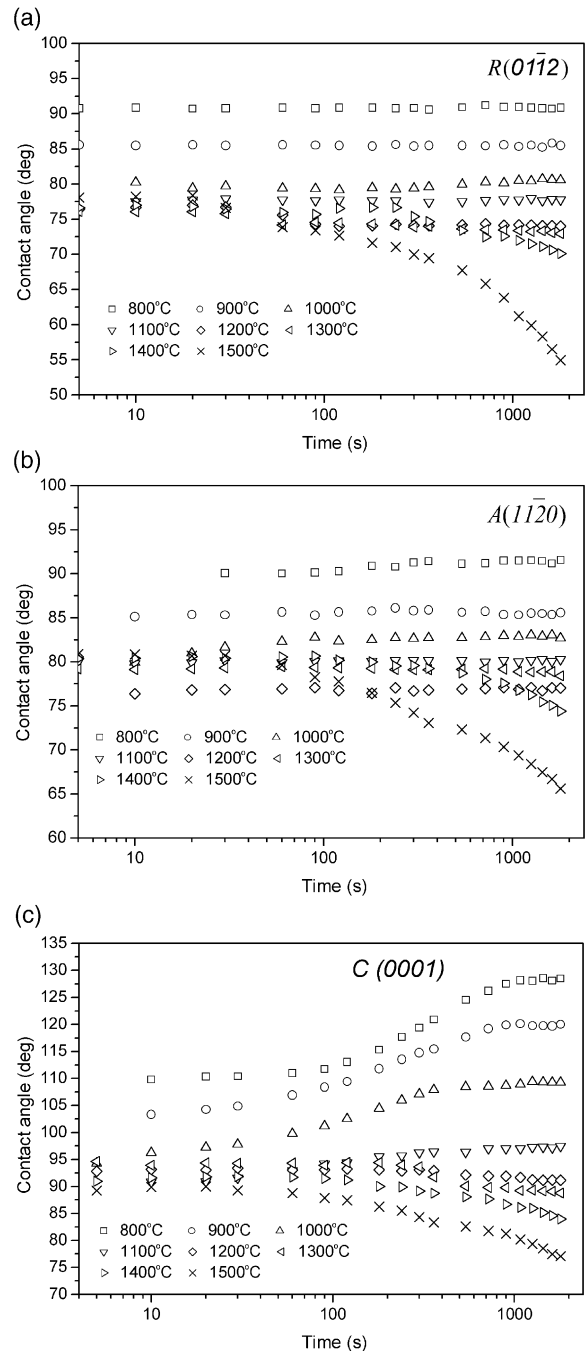


Fig. 3. Variations in contact angles of R (a), A (b), and C (c) single crystals with time at temperatures from 800–1500 °C as plotted on a logarithmic time scale.

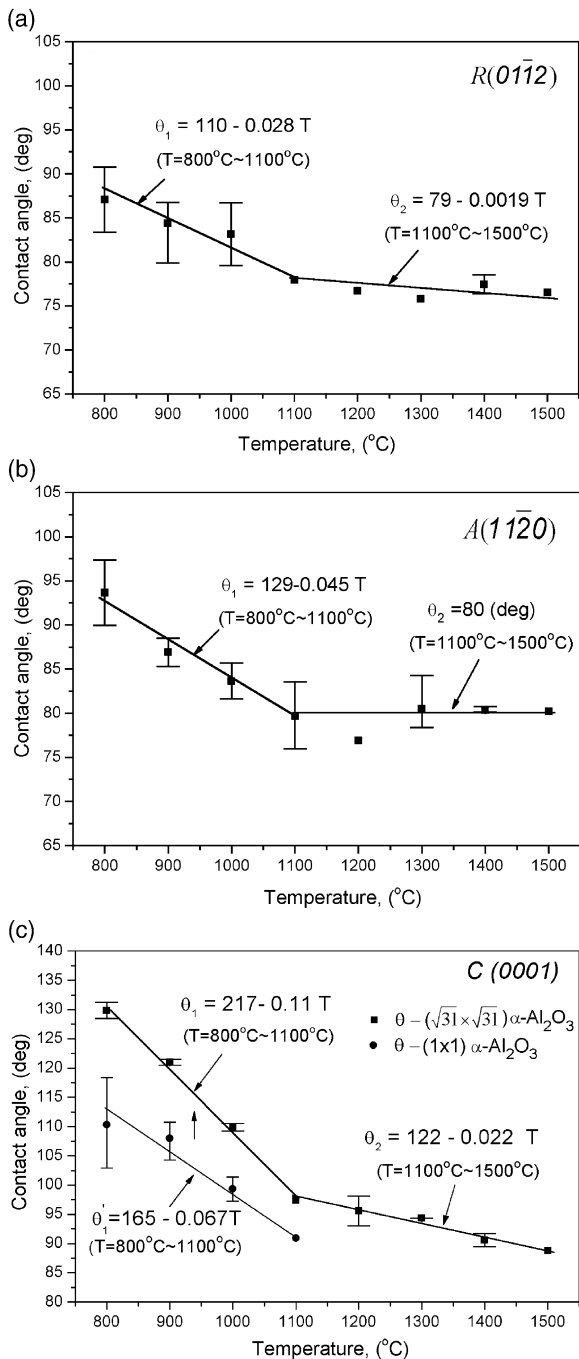


Fig. 4. Variations in the possibly true contact angles with temperature for R (a), A (b) and C (c) single crystals and their linear fit results.

the R and A faces (see Fig. 3), however, in different runs, their scatter is relatively large partly due to the different extents of the unavoidable surface oxidation under our experimental conditions or incompletely removed surface oxide when the liquid dropping from the alumina tube. At high temperatures, although the scatter in different runs is relatively smaller, the contact angles progressively decrease with time which results from the reaction between Al and Al_2O_3 at the interface. An increase in temperature significantly enhances the interfacial reaction. Measurement of the substrate surface profiles at the interface close to the triple junctions and microstructural observations indicate that at $T < 1100^\circ\text{C}$, no reaction rings but small wetting ridges [see Fig. 5(a)–(b)], whose height is on the order of 0.1–0.6 μm for temperatures at 900–1000 °C with an isothermal dwelling of 30 min, were detected at the triple junctions (Here, it is necessary for us to point out that the origin of the wetting ridges as described by Saiz et al. [34] is very different from that of the reaction rings as described by Champion et al. [35]). At $T = 1100\text{--}1200^\circ\text{C}$, both the wetting ridges and the reaction rings were found. However, the depths of the reaction rings are far less than 1 μm [see Fig. 5(c)–(d)]. At $T > 1200^\circ\text{C}$, however, the wetting ridges disappeared while the reaction rings developed to the depths ranging from about 1 μm for substrates at 1300 °C for 30 min to about 5.5 μm at 1400 °C for 30 min [see Fig. 5(e)–(f)]. Such deep valleys could produce a strong loss of the original orientation of the substrates and high deviation from the true contact angles defined by Young's equation since the interface close to the triple junctions is no longer straight and smooth, thus only the contact angles in the initial wetting periods are meaningful for reflecting the intrinsic wettability of $\alpha\text{-Al}_2\text{O}_3$ by molten Al at high temperatures. Furthermore, as seen from the high-temperature experiments with a long dwelling time, the decrease in contact angles may never end with a constant value [36]. Whereas, the maximum contraction angles, as observed in samples experiencing an alternating spread and contraction behavior (see Fig. 6), are close to those at 30 s (or near 30 s), indicating that the values at or near 30 s may represent the *true* contact angles for the Al/ $\alpha\text{-Al}_2\text{O}_3$ system while

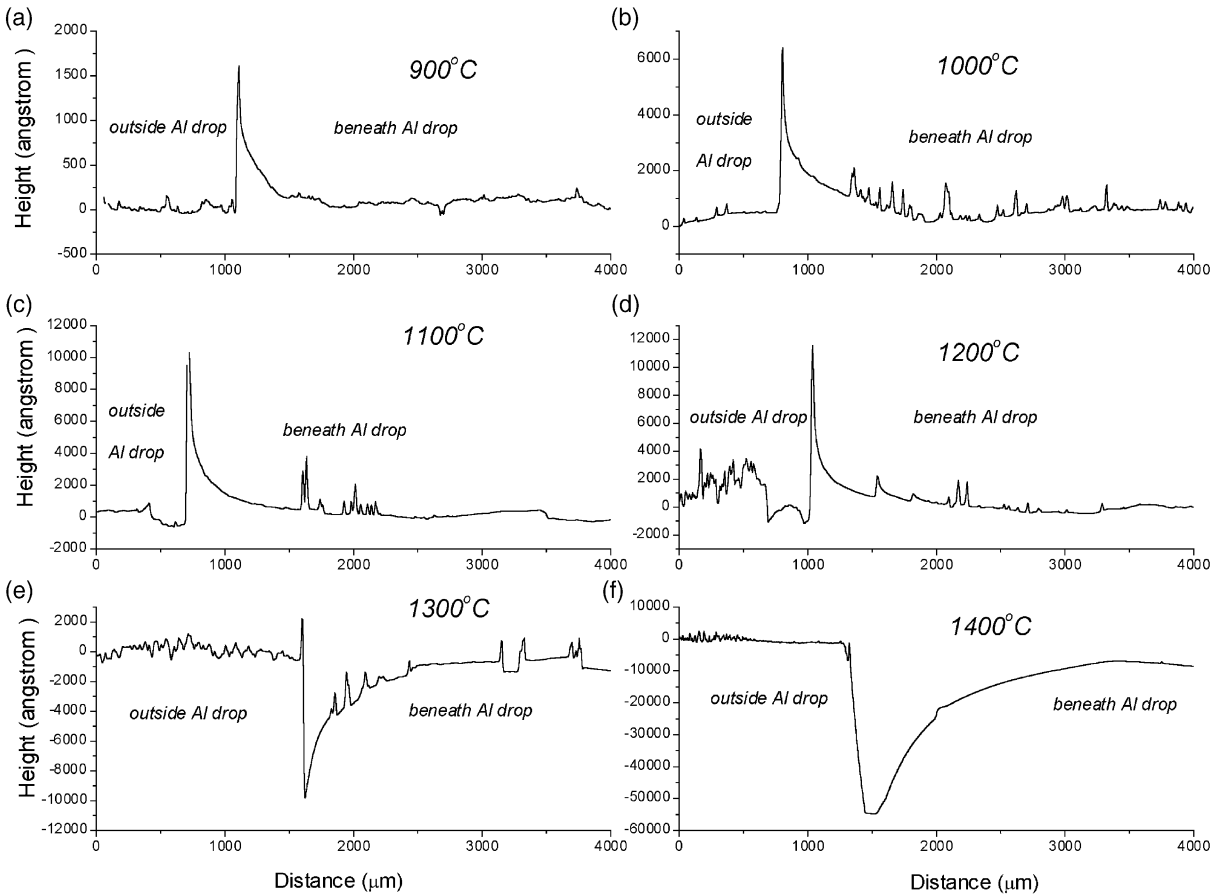


Fig. 5. Surface profiles in the vicinity of the triple junctions of the C-face α -Al₂O₃ substrates at the corresponding temperatures with a holding time of 30 min.

those progressively decreasing ones are the *apparent* contact angles.

As indicated in Figs. 3–4, the contact angles for the molten Al on the different oriented α -Al₂O₃ substrates are quite different, especially for the C face compared to the R and A faces, indicating that the wettability of α -Al₂O₃ by molten Al is sensitive to the substrate orientation in the reduced Ar-3%H₂ atmosphere. This result is completely different from the findings of Brennan et al. in vacuum [37] and Ownby et al. in a reduced H₂(He) atmosphere [38]. In their reports, the contact angles were concluded to be essentially independent of this parameter. Besides, from Fig. 4, it can be seen that the influence of the temperature on the wettability of all the α -Al₂O₃ single crystals by molten Al can

be roughly divided into two regions with $T = 1100$ °C as the boundary. At $T \leq 1100$ °C, the contact angles decrease relatively rapidly with temperature but do not significantly change with time except for the C face due to the surface structural reconstruction from (1×1) to $(\sqrt{3}1 \times \sqrt{3}1)R \pm 9^\circ$. The decreasing rate, i.e., the temperature coefficient of the contact angle, $d\theta/dT$, ranks C > A > R. At $T \geq 1100$ °C, the *true* contact angles decrease slowly or remain almost constant with temperature, whereas, the *apparent* contact angles decrease sharply at temperatures higher than 1300 °C [36]. The reason for the transition of the temperature dependence of the true contact angles at about 1100 °C is speculated to be related to the formation of the equilibrium structures on most R, A and C

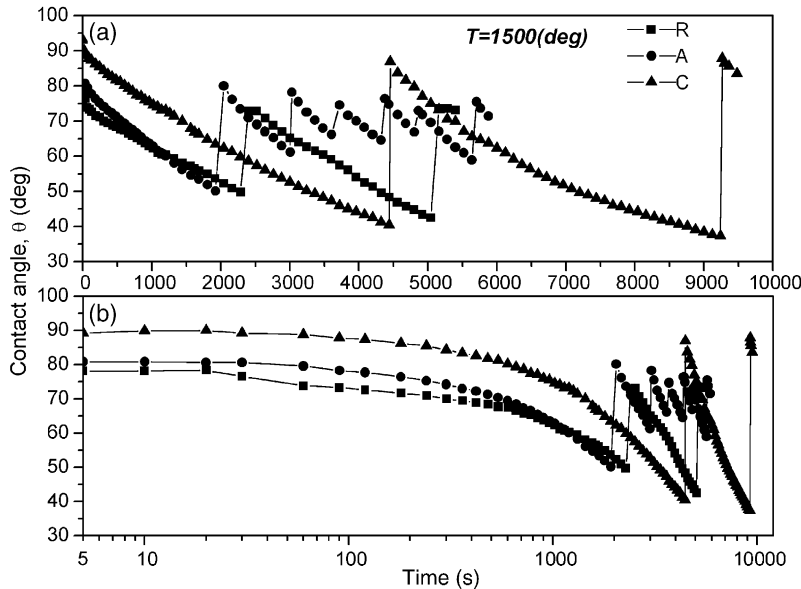


Fig. 6. Alternating spread and contraction of the contact angles in the R, A and C α -Al₂O₃ single crystals at 1500 °C. Note that the maximum contraction angles are close to the values at or near 30s, which is more clearly indicated in the logarithmic time scale graph (b).

surfaces as well as a rapid desorption of surface contaminants in the temperature range of 1000–1200 °C according to the observations of Chang [39] on the R, A and C surface structural and chemical changes during heat treatment using the LEED-Auger technique. Since the decreasing rate of the possibly true contact angles over the entire experimental temperature range is in the order of C > A ≥ R, they might be close to each other with a further increase in temperature.

The work of adhesion, W_{ad} , which is defined as the work required to separate a liquid from a solid, can be calculated using the Young-Dupré equation

$$W_{ad} = \sigma_{sg} + \sigma_{lg} - \sigma_{sl} = \sigma_{lg}(1 + \cos\theta) \quad (1)$$

where σ_{sg} , σ_{lg} and σ_{sl} are the solid-gas, liquid-gas and solid-liquid interfacial free energies, respectively, and θ is the *true* contact angle. Both σ_{lg} and θ are determined from our experiments. However, since the measured σ_{lg} values are relatively scattered in different runs of the experiments yet without an apparent relationship with the substrate orientation, their linear fit results are employed for calculation. The calculated results of W_{ad} are

shown in Fig. 7. It is clear that the values rank R ≥ A > C-(1 × 1) > C-($\sqrt{31} \times \sqrt{31}$)R ± 9°, especially at relatively low temperatures. Moreover, for the R and A faces, the values do not significantly change with temperature, while for the C face, they show a substantial increase, indicating that the interactions between molten Al and the C-

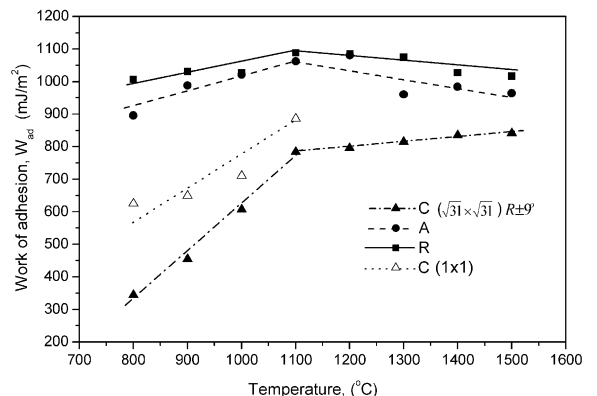


Fig. 7. The work of adhesion, W_{ad} , for molten Al on the R, A and C (including (1 × 1) and ($\sqrt{31} \times \sqrt{31}$)R ± 9°) α -Al₂O₃ single crystals at different temperatures.

face $\alpha\text{-Al}_2\text{O}_3$ surface strengthen as temperature increases.

4. Discussion

The wetting results of molten Al on the different oriented $\alpha\text{-Al}_2\text{O}_3$ single crystals are very interesting and provide some important information. However, in this article, we restrict ourselves to the topic of atomic termination (Al or O) at the top layer of the R, A and C surfaces.

The bonds at the Al/ $\alpha\text{-Al}_2\text{O}_3$ interface, as found in a recent first principles study [40], are very similar to the cation-anion bonds found in the oxide bulk and are mainly ionic yet maintain a small amount of covalent character. Therefore, the adhesion at the interface is similar to the cohesion in the $\alpha\text{-Al}_2\text{O}_3$ bulk and mainly depends on the Madelung energies, E_M , which involve the sum of the elementary coulomb interactions between pairs of ions (i, j) bearing charges Q_i and Q_j at a distance of R_{ij} [41]:

$$E_M = \frac{1}{2} \sum_{i \neq j} \frac{Q_i Q_j}{R_{ij}} \quad (2)$$

The primary interactions at the Al/ $\alpha\text{-Al}_2\text{O}_3$ interface are the Al-O bonds [40], i.e., the interactions between the molten Al atoms and the oxygen atoms of the $\alpha\text{-Al}_2\text{O}_3$ surface. For the simplest consideration, we assume that the oxygen atoms at the Al/ $\alpha\text{-Al}_2\text{O}_3$ interface are in the form of O^{2-} and the neighboring liquid aluminum atoms are in the form of Al^{3+} due to the Al-O bond, therefore, the work of adhesion can be expressed as

$$W_{\text{ad}} = k_1 E_M = \frac{N_1 \text{O}_{(s)}^{2-} \text{Al}_{(l)}^{3+}}{R_{\text{Al}(l)-\text{O}(s)}} \quad (3)$$

where k_1 is a proportionality constant, N_1 is the number of $\text{Al}_{(l)}-\text{O}_{(s)}$ bond pairs, depending on the quantity (or more exactly, the density) of the O^{2-} at the $\alpha\text{-Al}_2\text{O}_3$ surface, and $R_{\text{Al}(l)-\text{O}(s)}$ is the distance between O^{2-} and Al^{3+} at the interface (subscript l represents liquid state and s represents solid state). As a result, the value of W_{ad} is essentially dependent on the number of $\text{Al}_{(l)}-\text{O}_{(s)}$ bonds, i.e., the quantity/density of O^{2-} at the $\alpha\text{-Al}_2\text{O}_3$ surface,

particularly at the top layer of the surface, if the distance, $R_{\text{Al}(l)-\text{O}(s)}$, is assumed to be the same for all the Al/ $\alpha\text{-Al}_2\text{O}_3$ interfaces.

Note that in Fig. 7, $W_{\text{ad}}(\text{R}) \geq W_{\text{ad}}(\text{A}) > W_{\text{ad}}(\text{C}-(1 \times 1)) > W_{\text{ad}}(\text{C}-(\sqrt{31} \times \sqrt{31}))$. This is most favorable for the C face to be aluminum-terminated and the R and A faces to be oxygen-terminated if the combined termination is not considered here. Otherwise, if the C face is also oxygen-terminated, as seen from the surface atomic structure [1,42] and atomic stacking sequence [1,26,42] of these three $\alpha\text{-Al}_2\text{O}_3$ crystals (schematically shown in Fig. 8), one may draw the conclusion that $W_{\text{ad}}(\text{C})$ should be larger than both $W_{\text{ad}}(\text{R})$ and $W_{\text{ad}}(\text{A})$ because the quantity/density of O^{2-} at the top layers ranks $N_1(\text{C}) > N_1(\text{R}) > N_1(\text{A})$, which obviously contradicts our experimental results. Conversely, if it is terminated with aluminum, it is natural for $W_{\text{ad}}(\text{C})$ to be the smallest since the Al-Al bonds are much weaker than the Al-O bonds (The bond strengths of Al-Al and Al-O at 298K are $133 \pm 6 \text{ kJ mol}^{-1}$ and $511 \pm 3 \text{ kJ mol}^{-1}$, respectively [43]). Also, it is reasonable for the small difference between $W_{\text{ad}}(\text{R})$ and $W_{\text{ad}}(\text{A})$ due to an additional contribution of the oxygen in the second

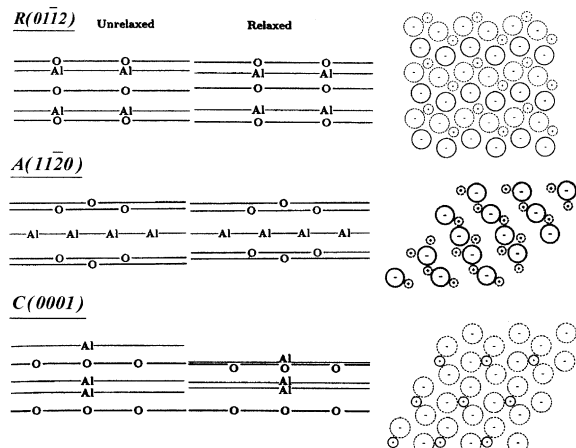


Fig. 8. Schematic representations of the atomic stacking sequences of the unrelaxed (left) and relaxed (middle) R, A and C $\alpha\text{-Al}_2\text{O}_3$ surfaces and the surface structures (right) [26,41]. The large circles represent O atoms, while the small ones represent Al atoms. The circles with straight line label the atoms at the top layer, while those with broken line label the atoms at the sub-layers. The atomic termination at the top layer of the above diagrams is based on assumption.

layer of the A surface with a relatively large distance, $R_{\text{Al(l)-O(s)}}$, if they are both terminated with oxygen at the top layer.

Furthermore, based on the result of the stronger adhesion on the unreconstructed C-(1 × 1) surface than that on the reconstructed C-($\sqrt{31} \times \sqrt{31}$)R ± 9° surface, we deduce that the latter must be a surface oxygen-deficient structure. This is easy to understand since there are only two elements in the Al_2O_3 crystal and the primary interactions at the interface are the $\text{Al}_{(l)}\text{-O}_{(s)}$ bonds. The deduction, although seemingly rather simple, is quite reasonable and consistent with the predictions from other surface analysis techniques, such as low-energy electron diffraction (LEED) [33], grazing incidence X-ray diffraction (GIXD) [3,44–45], X-ray photoemission spectroscopy (XPS) [46], and the density functional calculations [47].

On the other hand, if taking the empirical relationship of $W_{\text{ad}} \approx 0.2W_{c(l)}$ (where $W_{c(l)}$ is the cohesion of liquid metal and is equal to $2\sigma_{lg}$) as a typical characteristic of the physical interaction due to van der Waals dispersion forces, while $W_{\text{ad}} > 0.2W_{c(l)}$ as a chemical interaction in nature [48–49], we can also infer from Fig. 9 that the interactions on the R and A surfaces are always chemical, i.e., from the $\text{Al}_{(l)}\text{-O}_{(s)}$ bonds at the interface, while on the C surface, the interactions change from physical to chemical, i.e., from the Al-Al bonds to the Al-O bonds as the temperature increases. This is specific for the reconstructed C-

($\sqrt{31} \times \sqrt{31}$)R ± 9° surface. For the relaxed yet unreconstructed C-(1 × 1) surface, the interactions are combined with physical and chemical forces due to the large inward relaxation of the top layer Al atoms [4,26–27] as illustrated in Fig. 8, leading to the under-layer oxygen atoms being very close to the top surface, and hence a significant decrease in $R_{\text{Al(l)-O(s)}}$ between the under-layer oxygen atoms and the molten Al atoms at the interface and an increase in the interfacial bonds.

5. Conclusions

The wetting of molten Al on three different oriented $\alpha\text{-Al}_2\text{O}_3$ single crystals, R (011̄2), A(11̄20) and C (0001), in the reduced Ar-3%H₂ atmosphere was studied over the wide temperature range of 800–1500 °C using an improved sessile drop method. It was found that the wettability and adhesion between the molten Al and the $\alpha\text{-Al}_2\text{O}_3$ surfaces are quite sensitive to the crystallographic orientation. The adhesion is much stronger for molten Al on the R and A surfaces than that on the C surface. On the other hand, the adhesion on the reconstructed C-($\sqrt{31} \times \sqrt{31}$)R ± 9° surface is weaker than that on the relaxed yet unreconstructed C-(1 × 1) surface. Therefore, based on the results of the work of adhesion, it is deduced that in the Ar-3%H₂ atmosphere, the top layers of the R and A surfaces are oxygen-terminated while that of the C surface is aluminum-terminated, and the reconstructed C-($\sqrt{31} \times \sqrt{31}$)R ± 9° surface is an oxygen-deficient structure.

As a general conclusion, we suggest that the wetting experiment sometimes could also be an effective means for analyzing the surface structure at high temperatures by employing a specified system in a controlled atmosphere.

Acknowledgements

This work is supported by the International Joint Research Grant Program from the New Energy and Industrial Technology Development Organization (NEDO) of Japan, and also by the Priority Assistance of the Formation of Worldwide Renowned

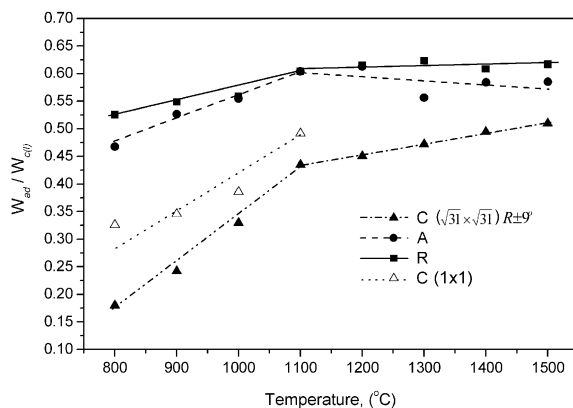


Fig. 9. Calculated results of $W_{\text{ad}}/W_{c(l)}$ for molten Al on the R, A and C (with two structures) single crystals at different temperatures.

Centers of Research—The 21st Century COE Program (Project: Center of Excellence for Advanced Structural and Functional Materials Design) from the Ministry of Education, Sports, Culture, Science and Technology of Japan.

References

- [1] Henrich VE, Cox PA. *The surface science of metal oxides*. Cambridge: Cambridge Univ. Press, 1994.
- [2] French RH, Heuer AH. *J Am Ceram Soc* 1994;77:292.
- [3] Gautier M, Renaud G, Pham Van L, et al. *J Am Ceram Soc* 1994;77:323.
- [4] Ahn J, Rabalais JW. *Surf Sci* 1997;388:121.
- [5] Guo J, Ellis DE, Lam DJ. *Phy Rev B* 1992;45:13647.
- [6] Soares EA, Van Hove MA, Walters CF, Mcdarty KF. *Phy Rev B* 2002;65:195405.
- [7] Guénard P, Renaud G, Barbier A, Gautier-Soyer M. *Surf Rev Lett* 1997;5:321.
- [8] Godin TJ, Femina JPLA. *Phy Rev B* 1994;49:7691.
- [9] Suzuki T, Hishita S, Oyoshi K, Souda R. *Surf Sci* 1999;437:289.
- [10] TePesch PD, Quong AA. *Phys Stat Sol (b)* 2000;217:377.
- [11] Batyrev I, Alavi A, Finnis MW. *Faraday Discuss* 1999;114:33.
- [12] Ciraci S, Batra IP. *Phy Rev B* 1983;28:982.
- [13] Wei PSP, Smith AW. *J Vac Sci Technol* 1972;9:1209.
- [14] Arbab M, Chottiner GS, Hoffman RW. *Mater Res Soc Symp Proc* 1989;153:63.
- [15] Jaeger RM, Kuhlenbeck H, Freund HJ, et al. *Surf Sci* 1991;259:235.
- [16] Guglielmacci J-M, Ealet B. *Mater Sci Eng B* 1996;40:96.
- [17] Heffelfinger JR, Bench MW, Carter CB. *Surf Sci* 1997;370:L168.
- [18] Toofan J, Watson PD. *Surf Sci* 1998;401:162.
- [19] Liu P, Kendelewicz T, Brown Jr GE, Nelson EJ, Chambers SA. *Surf Sci* 1998;417:53.
- [20] Eng PJ, et al. *Science* 2000; 288(12):1029.
- [21] Wang XG, Chaka A, Scheffler M. *Phys Rev Lett* 2000;84:3650.
- [22] Barth C, Reichling M. *Nature* 2001;414:54.
- [23] Felice RD, Northrup JE. *Phys Rev B* 1999;60:16287.
- [24] Gignac WJ, Williams RS, Kowalczyk SP. *Phy Rev B* 1985;32:1237.
- [25] Nogi K, Nishikawa M, Fujii H, Hara S. *Acta Metall Mater* 1998;46:2305.
- [26] Manassisidis I, Gillan MJ. *J Am Ceram Soc* 1994;77:335.
- [27] Puchin VE, Gale JD, Shluger AL, et al. *Surf Sci* 1997;370:190.
- [28] Nogi K, Ogino K. *Can Inst Mine Metall* 1983;22:19.
- [29] Fujii H, Nakae H, Okada K. *Acta Metall* 1993;41:2963.
- [30] Fujii H, Shiraki A, Kohno M, Matsumoto T, Nogi K. Measurements of silicon surface tension using the oscillating drop method and the sessile drop method. In: Eustathopoulos N, Nogi K, Sobczak N, editors. *Proc Int Conf High Temperature Capillarity*, 19–22 Nov, 2000, Kurashiki, Japan; 2001, p. 275.
- [31] Fujii H, Matsumoto T, Hata N, Nakano T, Kohno M, Nogi K. *Metall Mater Trans A* 2000;31A:1586.
- [32] Shen P, Fujii H, Matsumoto T, Nogi K. *Scripta Mater* 2003;48(6):779.
- [33] French TM, Somorjai GA. *J Phys Chem* 1970;74:2489.
- [34] Saiz E, Tomsia AP, Cannon RM. *Acta mater* 1998;46(7):2349.
- [35] Champion JA, Keen BJ, Sillwood JM. *J Mater Sci* 1969;4:39.
- [36] Shen P, Fujii H, Matsumoto T, Nogi K. *Scripta Mater*, 2003;49(6):563.
- [37] Brennan JJ, Pask JA. *J Am Ceram Soc* 1968;51:569.
- [38] Ownby PD, Li Ke Wen K, Weirauch Jr. DA. *J Am Ceram Soc* 1991;74:1275.
- [39] Chang CC. *J Vac Sci Technol* 1971;8(3):500.
- [40] Siegel DJ, Hector Jr LG, Adams JB. *Phys Rev B* 2002;65:085415.
- [41] Noguera C. *Physics and chemistry at oxide surfaces*. Cambridge: Cambridge Univ. Press, 1996.
- [42] Tasker PW. *Surface of magnesia and alumina*. In: Kingry WD, editor. *Structure and Properties of MgO and Al₂O₃ Ceramics*. The American Ceramic Society; 1984. p. 17–6.
- [43] Kerr JA. Strengths of chemical bonds. In: Lide DR, Frederikse HPR, editors. *CHC Handbook of Chemistry and Physics* 1995–1996. 76th ed. CRC press; 1995. p. 199–5.
- [44] Renaud G. *Surf Sci Reports* 1998;32:1
- [45] Renaud G, Villette B, Vilfan I, Bourret A. *Phys Rev Lett* 1994;73:1825.
- [46] Varma S, Chottiner GS, Arbab M. *J Vac Sci Technol* 1992;10(4):2857.
- [47] Jarvis EAA, Carter EA. *J Phys Chem B* 2001;105:4045.
- [48] Naidich YV. The wettability of solids by liquid metals. In: Cadenhead DA, Danielli JF, editors. *Progress in Surface and Membrane Science*, vol. 14. New York: Academic Press; 1981. p. 353.
- [49] Eustathopoulos N, Nicholas MG, Drevet B. *Wettability at high temperatures*. Oxford, UK: Pergamon, Elsevier Science, 1999.